

# Angularly resolved light scattering from aerosolized spores: observations and calculations

Jean-Claude Auger,<sup>1</sup> Kevin B. Aptowicz,<sup>2,\*</sup> Ronald G. Pinnick,<sup>3</sup> Yong-Le Pan,<sup>1</sup> and Richard K. Chang<sup>1</sup>

<sup>1</sup>Department of Applied Physics, Yale University, New Haven, Connecticut 06520, USA

<sup>2</sup>Department of Physics, West Chester University, West Chester, Pennsylvania, 19383, USA

<sup>3</sup>U.S. Army Research Laboratory, Adelphi, Maryland 20783, USA

\*Corresponding author: kaptowicz@wcupa.edu

Received September 18, 2007; accepted October 4, 2007;  
posted October 25, 2007 (Doc. ID 87689); published November 14, 2007

Angularly resolved elastic light scattering patterns from individual aerosolized *Bacillus subtilis* spores were qualitatively compared with simulations. Two-dimensional angular optical scattering patterns of the spores were collected for polar scattering angles varying from approximately  $77^\circ$  to  $130^\circ$  and azimuthal angles varying from  $0^\circ$  to  $360^\circ$ . Computations were performed with single T-matrix formalism by simulating a spore with three different particle shapes: (1) a finite-length cylinder with spherical end caps, (2) a spheroid, and (3) two spheres in contact. Excellent agreement between computation and measurement was found for the finite-length cylinder with spherical end caps, poorer agreement was found for the spheroids, and the poorest agreement was for the two spheres in contact. © 2007 Optical Society of America

OCIS codes: 290.5850, 290.3200, 290.1090.

Characterization of airborne particles such as allergens, pathogens, or biological warfare agents is of great importance for civil and military purposes. Using microphotography, it is not possible to record, on-the-fly, direct optical images of such particles, which range from  $0.1$  to  $10.0 \mu\text{m}$ . On the other hand, images of angularly resolved elastically scattered light from single aerosol particles provide one possible approach for *in situ* and real-time identification [1–5]. Here we show that the combination of the experimental setup we developed [6,7] and the theoretical analysis we implemented allows for the characterization of aerosolized nonspherical particles with great precision. In particular, we collected the two-dimensional angular optical scattering (TAOS) patterns of a single *Bacillus subtilis* (BG) spore that is commonly used as a simulant for the *Bacillus anthracis* bacteria. High-resolution scattering images ( $1024 \times 1024$  pixels) collected using the TAOS technique spanned polar scattering angles ( $\theta$ ) varying from approximately  $77^\circ$  to  $130^\circ$  and azimuthal angles ( $\phi$ ) varying from  $0^\circ$  to  $360^\circ$ . Precise numerical replicas of those patterns are generated using single T-matrix formalism. Finally, we illustrate that the selected geometry to represent the particle's shape is a primordial parameter in the calculations, which greatly affects the agreement with experimental data.

The experimental setup to obtain TAOS patterns has been previously described [6]. A dilute suspension of BG spores was aerosolized using a nebulizer (Royco Aerosol Generator, Model 256) generating single airborne spores that were then introduced into the inlet of the instrument. We found that this technique of aerosolization is superior to a previously used technique [7,8] because it minimizes the contributions of other materials, such as surfactant, to the surface of the spore. This improvement led to TAOS

patterns of BG spores that were more accurate than have been previously detected. Figure 1 shows four TAOS patterns captured from four separate BG spores flowing through the system. The scattered intensity was plotted on a logarithmic scale because the amplitude of the intensities in the forward and backward regions can differ by several orders of magnitude. The maximum scattered intensity is coded white to increase the readability of the TAOS patterns. The pulsed Nd:YAG laser ( $0.532 \mu\text{m}$  wavelength) beam traveling in a horizontal plane is defined as the  $z$ -axis and is linearly polarized in the vertical direction. The outer circumference of the image corresponds to light scattered at  $\theta = 77^\circ$  with re-

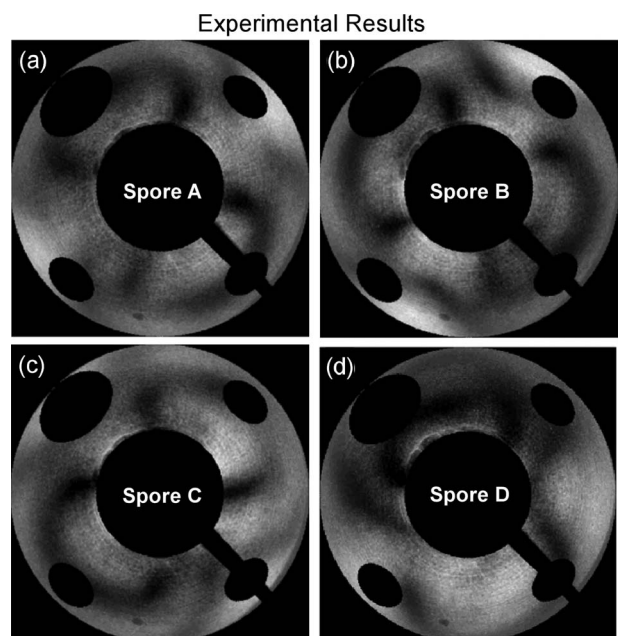


Fig. 1. Experimental TAOS patterns collected for different BG spores.

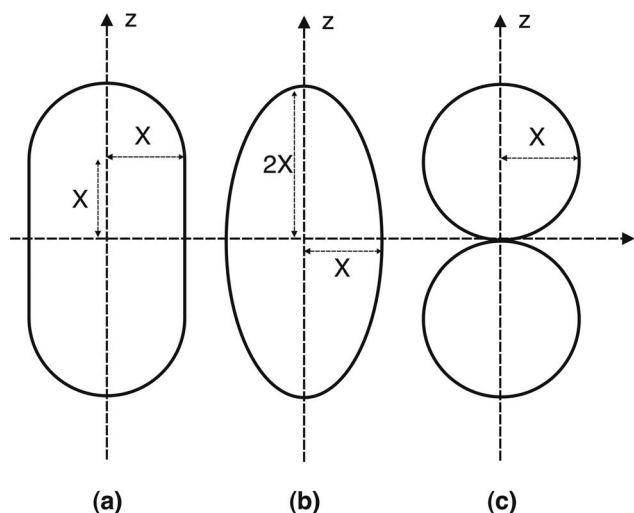


Fig. 2. Selected geometries to model the shape of the BG spores: (a) finite cylinder covered by two hemispheres, (b) prolate spheroid, and (c) two spheres in contact.

spect to the laser beam's propagation axis; the inner circumference corresponds to light scattered at  $\theta = 130^\circ$ .

There are several experimental artifacts in the TAOS patterns. Holes are drilled in the ellipsoidal collection mirror for one of the trigger beams as well as the particle-laden air stream that appear as off-centered ovals in the patterns. A mounting post used to hold a beam-steering mirror appears as a black bar on the bottom right of the images. BG spores have a nonspherical structure, thus the TAOS patterns are expected to vary with particle's orientation. We believe that the major cause of the variability among these TAOS patterns presented in Fig. 1 is due to changes in particle orientation rather than significant changes in the shape or size of the spores. In particular, the orientations of the individual spores' long axis relative to the  $z$ -axis and polarization of the incident laser beam will be referred to afterward as  $\beta$  and  $\alpha$ , respectively. Note the mirror symmetry present in some of the patterns that occurs when aerodynamic forces on the particle align the particle's long axis in the direction of airflow, which is perpendicular to the incident laser beam ( $\beta = 90^\circ$ ).

Based on observations of scanning electron microscope images we modeled the shape of the spores as finite-length cylinders covered by two spherical caps whose global aspect ratio is about 2, shown in Fig. 2(a). Such a geometry allowed characterizing the overall particle by a single dimension, noted  $X$ , and is a reasonable approximation of the actual spore shape. Thereby each simulation can be uniquely characterized by the knowledge of the three "triplet" parameters  $X$ ,  $\beta$ , and  $\alpha$ . The numerical study was based on single T-matrix formalism [9], which allowed taking advantage of the axial symmetry of the particle. Calculations were performed on a simple desktop computer via a FORTRAN 90 code that we previously developed and carefully validated with published data [10]. The spores were assumed to be homogeneous with the refractive index at the wavelength of the laser,  $1.52 + i0.018$  [11]. The ranges of

polar and azimuthal observation angles were varied to match the experiment.

The analysis and identification processes between measured and calculated TAOS patterns were based on visual comparisons. Figure 3 shows examples of numerical replicates of the measured TAOS patterns illustrated in Fig. 1. Visual examination clearly shows that our calculations reproduce with relatively precise detail the structures of the experimental patterns. In particular, the shapes and relative intensities associated with the two minimum lines of the scattered intensity in the shape of an "eight." It must be pointed out that, rather than a single absolute replicate, each experimental TAOS pattern can be related to an ensemble of simulated patterns whose visual analysis leads to "fair" comparison. As an example, the simulations that lead to the fairly good comparisons with experimental TAOS shown in Fig. 1(d) have their triplets ranging in the intervals  $\Delta X$ ,  $\Delta\beta$ , and  $\Delta\alpha$  such that  $0.310 \leq X \leq 0.320$ ,  $65^\circ \leq \beta \leq 75^\circ$ , and  $0^\circ \leq \alpha \leq 10^\circ$ . Within these ranges, it is not possible to clearly distinguish among all simulations which one leads to the optimum replicate. In addition, slight changes in the global aspect ratio of the particle shape did not improve the quality of the simulations.

To investigate the variations of the calculated TAOS patterns by changing the particle's geometry, we carried out two additional comparative studies in which the BG spore was modeled as a spheroid and two spheres that were in contact as shown in Figs. 2(b) and 2(c) [12]. In the present work, simulations of the bisphere particles were performed via the recursive centered T-matrix algorithm, whose comprehensible description and cautious validation have been presented in the literature [13]. Systematic calcula-

Numerical Results - Cylinder with Spherical End Caps

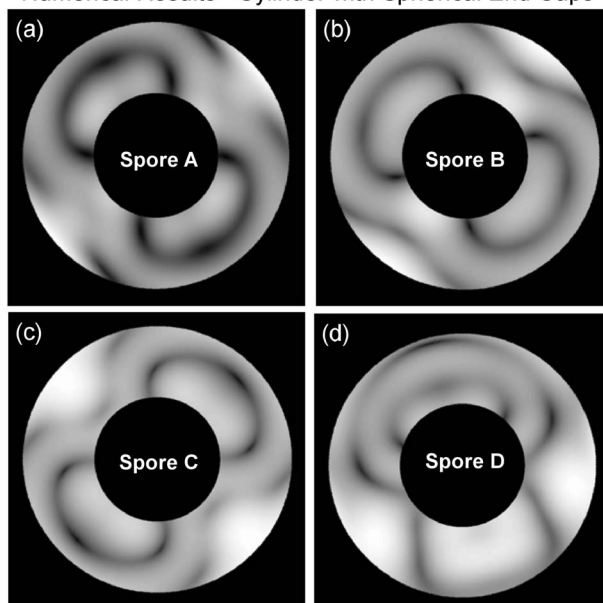


Fig. 3. Theoretical replicates of the TAOS patterns shown in Fig. 1. The spore is modeled as shown in Fig. 2(a) with (a)  $X = 0.325 \mu\text{m}$ ,  $\beta = 90^\circ$ ,  $\alpha = 60^\circ$ ; (b)  $X = 0.316 \mu\text{m}$ ,  $\beta = 90^\circ$ ,  $\alpha = 10^\circ$ ; (c)  $X = 0.325 \mu\text{m}$ ,  $\beta = 90^\circ$ ,  $\alpha = 10^\circ$ ; and (d)  $X = 0.316 \mu\text{m}$ ,  $\beta = 70^\circ$ ,  $\alpha = 0^\circ$ .

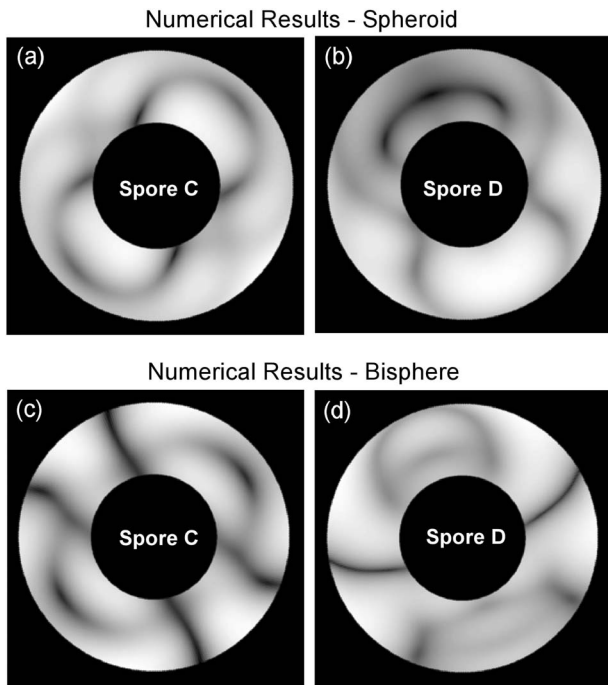


Fig. 4. (a) and (b) Replicates of Figs. 1(c) and 1(d), respectively, modeling the spore shape as a prolate spheroid. (c) and (d) Replicates Figs. 1(c) and 1(d), respectively but modeling the spore shape as two spheres in contact.

tions were performed on all possible orientations of the spore with respect to the wave vector and polarization of the incident radiation and the characteristic parameter  $X$  ranged from 0.250 to 0.450  $\mu\text{m}$ .

The quality of the TAOS patterns calculated with the spheroidal particles varied slowly as function of the orientation of the particle with respect to the incident wave vector direction. In the case of perpendicular incidence ( $\beta=90^\circ$ ), the shape of the first minimum line was only vaguely reproduced; in addition, the curvatures of the second minima could not be adjusted to fit the measurements. An example of an attempt to reproduce the experiment pattern appearing in Fig. 1(c) is shown in Fig. 4(a). We note that when the wave vector of the incident radiation struck the spore with an oblique incidence ( $\beta \neq 90^\circ$ ), the similarity of the replicates was greatly improved [see Fig. 4(b) as a replicate of Fig. 1(d)]. However, overall, the quality of the replicates was not as good as that obtained when modeling the spore by a finite-length cylinder with spherical end caps. Furthermore, simulations using the bisphere systems were always largely erroneous, as shown in Fig. 4(c) as a replicate of in Fig. 1(c) and in Fig. 4(d) as a replicate of Fig. 1(d).

In summary, using the single T-matrix formalism, we have been able to replicate the experimental TAOS patterns of aerosolized BG spores by modeling their shape as a homogeneous finite-length cylinder

with spherical end caps. These results provide evidence that electromagnetic theories can successfully characterize TAOS patterns of nonspherical biological objects with size parameters ranging from 5 to 7. Such an achievement was made possible because of the high-resolution CCD camera used in this experiment and the computational approach to solving the solution and displaying the results in the same way as the experimental results. Therefore, a detailed comparison can be made between computational and experimental TAOS images. This study reveals clearly strong variation in the computed TAOS patterns that is dependent on the selected geometry to represent the spore. In particular, the finite-length cylinder with spherical end caps model for BG spores agrees well with the experimental TAOS patterns. By assuming spheroidal geometry for BG spores, calculations showed a less accurate replicate of the measured TAOS patterns. Assuming a bisphere geometry [12] for BG spores gave an even worse agreement with experimental TAOS patterns. Finally, we expect that this confluence of advances in computational modeling and electro-optic devices will provide a platform that enables characterization of single airborne particles in different fields of research such as health science and national security.

Army Research Laboratory machinist John Bowersett machined the aerosol inlet nozzle for the TAOS experimental setup.

## References

1. F. T. Gucker, J. Tuma, H.-M. Lin, C.-M. Huang, S. C. Ems, and T. R. Marshall, *J. Aerosol Sci.* **4**, 389 (1973).
2. P. J. Wyatt, K. L. Schehrer, S. D. Phillips, C. Jackson, Y. J. Chang, R. G. Parker, D. T. Phillips, and J. R. Bottiger, *Appl. Opt.* **27**, 217 (1988).
3. E. Hirst and P. H. Kaye, *J. Geophys. Res.* **101**, 19231 (1996).
4. C. Li, G. W. Kattawar, and P. Yang, *Opt. Express* **14**, 3616 (2006).
5. D. Petrov, G. Videen, Y. Shkuratov, and M. Kaydash, *J. Quant. Spectrosc. Radiat. Transf.* **108**, 81 (2007).
6. K. B. Aptowicz, R. G. Pinnick, S. C. Hill, Y. L. Pan, and R. K. Chang, *J. Geophys. Res.* **111**, D12212 (2006).
7. Y.-L. Pan, K. B. Aptowicz, R. K. Chang, M. Hart, and J. D. Eversole, *Opt. Lett.* **28**, 589 (2003).
8. G. E. Fernandes, Y. L. Pan, R. K. Chang, K. Aptowicz, and R. G. Pinnick, *Opt. Lett.* **31**, 3034 (2006).
9. M. I. Mishchenko, L. D. Travis, and A. A. Lacis, *Scattering, Absorption and Emission of Light by Small Particles* (Cambridge U. Press, 2002).
10. M. I. Mishchenko, *J. Opt. Soc. Am. A* **8**, 871 (1991).
11. P. S. Tuminello, E. T. Arakawa, B. N. Khare, J. M. Wrobel, M. R. Querry, and M. E. Milham, *Appl. Opt.* **36**, 2818 (1997).
12. O. I. Sindoni, R. Saija, M. A. Iati, F. Borghese, P. Denti, G. E. Fernandes, Y.-L. Pan, and R. K. Chang, *Opt. Express* **14**, 6942 (2006).
13. J. C. Auger and B. Stout, *J. Quant. Spectrosc. Radiat. Transf.* **79-80**, 533 (2003).